

Supplementary Information

Study of the impact of long-duration space missions at the International Space Station on the astronaut microbiome

Alexander A. Voorhies¹, C. Mark Ott², Satish Mehta², Duane L. Pierson², Brian E. Crucian², Alan Feiveson², Cherie M. Oubre², Manolito Torralba¹, Kelvin Moncera¹, Yun Zhang¹, Eduardo Zurek⁴, and Hernan A. Lorenzi^{1*}.

1. Department of Infectious Diseases, J. Craig Venter Institute, Rockville MD, USA
2. NASA-Johnson Space Center, Houston TX, USA
3. Universidad del Norte, Barranquilla, Colombia

* Materials and corresponding author:

Email: hlorenzi@jcvj.org
The J. Craig Venter Institute
9605 Medical Center Drive
Suite 150
Rockville, MD 20850

Supplementary figure legends

Figure S1: principal coordinate plots of unweighted Bray-Curtis beta diversity distances across all samples collected in the study. A, samples coloured by body or ISS surface site. The permanova p-value using body site as the independent variable is shown. B, human microbiome samples coloured by astronaut identifier. Each microbiome is represented with a different symbol. Permanova p-value and R² using astronaut identifier as the independent variable and stratifying by body site are indicated.

Figure S2: comparative analysis of beta diversity distances among microbial communities collected from the same or different crew members. Boxplot of weighted (A-E) and unweighted (F-J) Bray-Curtis beta diversity distances between samples collected from the same (Intra) or different (Inter) astronauts. The Welch two-sample t-test p-values of the comparison of Inter- versus Intra-astronaut distances are indicated.

Figure S3: comparative beta diversity analysis among ISS microbial communities and nose, forehead and forearm skin microbiomes. Principal coordinate analysis of weighted (top panels) and unweighted (bottom panels) Bray-Curtis beta diversity among ISS environmental microbiota and forearm (A and D), forehead (B and E) and nose (C and F) microbiomes. Red circles, crew inflight samples; blue circles, crew pre and postflight samples; green circles, ISS environmental samples. Permanova p-values and R² values are indicated.

Figure S4: changes in alpha diversity and richness of individual crew members during a mission at the ISS. Boxplots depicting changes in Shannon alpha diversity (A) and Richness (B) of the five human microbiomes surveyed, by individual astronaut. Microbiome source is indicated on the right.

Figure S5: differential response of the astronauts' skin microbiota to the space environment. Boxplots depicting opposed responses of the skin microbiome to spaceflight. The forehead and forearm skin of astronauts A, B, D, F and H showed an increase in both Shannon alpha diversity (A) and species Richness (B) during spaceflight, while the same two skin sites of astronauts C, E, G and I responded in the opposite direction during spaceflight. Linear mixed-effects model p-values ≤ 0.06 are depicted using Preflight samples as a baseline.

Figure S6: compositional changes in the astronauts' microbiome during a space mission. Differences in the mean weighted (A) and unweighted (B) Bray-Curtis beta diversity distance between samples collected at individual inflight (blue) or postflight (yellow) time points and preflight samples. Grey boxplots represent the average within-astronaut weighted (A) or unweighted (B) Bray-Curtis distance among all preflight samples. Linear mixed-effects model p-values ≤ 0.05 are shown using within-preflight distances as baseline.

Figure S7: comparative analysis of inter-astronaut beta diversity distances of the GI microbiome before, during and after a space mission. A, Principal coordinate plot of weighted Bray-Curtis beta diversity distances among GI microbiome samples collected during preflight (blue) or inflight (red) stages. Astronauts B, C, D, F and G are represented with distinct symbols. B, boxplot showing that the weighted Bray-Curtis distance between GI samples from distinct crew members becomes smaller in the ISS compared to preflight samples. The Welch two-sample t-test p-values of the comparison between preflight distances versus inflight or postflight distances are shown.

Figure S8: changes in the relative abundance of bacterial genera of the astronauts' forehead skin during a mission at the ISS and after the return to Earth. Colours represent different phyla; horizontal axis, logarithm of the fold change in relative abundance between preflight and inflight or postflight samples; vertical axis, bacterial genera. Black circles indicate genera belonging to the corresponding preflight core microbiome.

Figure S9: bacterial genera of the GI microbiome that present the largest absolute difference between preflight and inflight coefficients of variation (CV) of their relative abundance across astronauts. Yellow bars indicate bacterial genera whose relative abundance becomes more similar in the ISS ($CV_{\text{preflight}} >$

CV_{inflight}), while Blue bars represent those genera whose abundance becomes more different in space (CV_{preflight} < CV_{inflight}).

Figure S10: changes in beta diversity of the environmental microbiome of the ISS. Principal coordinate plots of weighted (A and B) and unweighted (C and D) Bray-Curtis distances depicting shifts in the composition of the ISS microbiome across ISS surfaces (A and C) and over time (B and D). Panels A and C, distinct ISS surfaces are represented by different colours. Panels B and D, colours and numbers represent distinct relative mission time points, as indicated in Fig. 1B. Ellipses represent 95% confidence intervals. Permanova p-values < 0.05 and R² values are shown.

Figure S11: comparative analysis of alpha diversity and richness across inflight skin and ISS environmental samples. Boxplots depicting Shannon alpha diversity (A) and Richness (B) of inflight forehead and forearm skin samples and of the six ISS surfaces surveyed in this study.

Figure S12: bubble plot showing changes in the relative abundance of OTUs ubiquitously detected on ISS surface ssA during the entire study. Circle sizes are proportional to the relative abundance of each OTU at every relative time point. For each OTU, phylum and genus are indicated. No sample was collected at relative mission time 10.

Figure S13: bubble plot showing changes in the relative abundance of OTUs ubiquitously detected on ISS surface ssB during the entire study. Circle sizes are proportional to the relative abundance of each OTU at every relative time point. For each OTU, phylum and genus are indicated. No sample was collected at relative mission time 10.

Figure S14: bubble plot showing changes in the relative abundance of OTUs ubiquitously detected on ISS surface ssC during the entire study. Circle sizes are proportional to the relative abundance of each OTU at every relative time point. For each OTU, phylum and genus are indicated. No sample was collected at relative mission time 10.

Figure S15: bubble plot showing changes in the relative abundance of OTUs ubiquitously detected on ISS surface ssD during the entire study. Circle sizes are proportional to the relative abundance of each OTU at every relative time point. For each OTU, phylum and genus are indicated. No sample was collected at relative mission time 10.

Figure S16: bubble plot showing changes in the relative abundance of OTUs ubiquitously detected on ISS surface ssF during the entire study. Circle sizes are proportional to the relative abundance of each OTU at every relative time point. For each OTU, phylum and genus are indicated. No sample was collected at relative mission time 10.

Figure S17: bubble plot showing changes in the relative abundance of OTUs ubiquitously detected on the ISS surface ssE during the entire study. Circle sizes are proportional to the relative abundance of each OTU at every relative time point. For each OTU, phylum and genus are indicated. No sample was collected at relative mission time 10.

Figure S18: detection of viral DNA and stress hormones in saliva. A-C, qPCR detection of HSV1 (A), EBV (B) and VZV (C) genomic DNA in astronauts' saliva during a mission at the ISS and after their return to Earth. Red line, mean viral DNA concentration in saliva across all virus-positive crewmembers. Dotted lines, viral DNA concentration levels for individual astronauts. D-F, changes in the concentration of alpha amylase (D), DHEA (E) and cortisol (F) in astronauts' saliva. Significance is depicted for mean values only. o, p-value < 0.1; *, p-value < 0.05; **, p-value < 0.01.

Figure S1

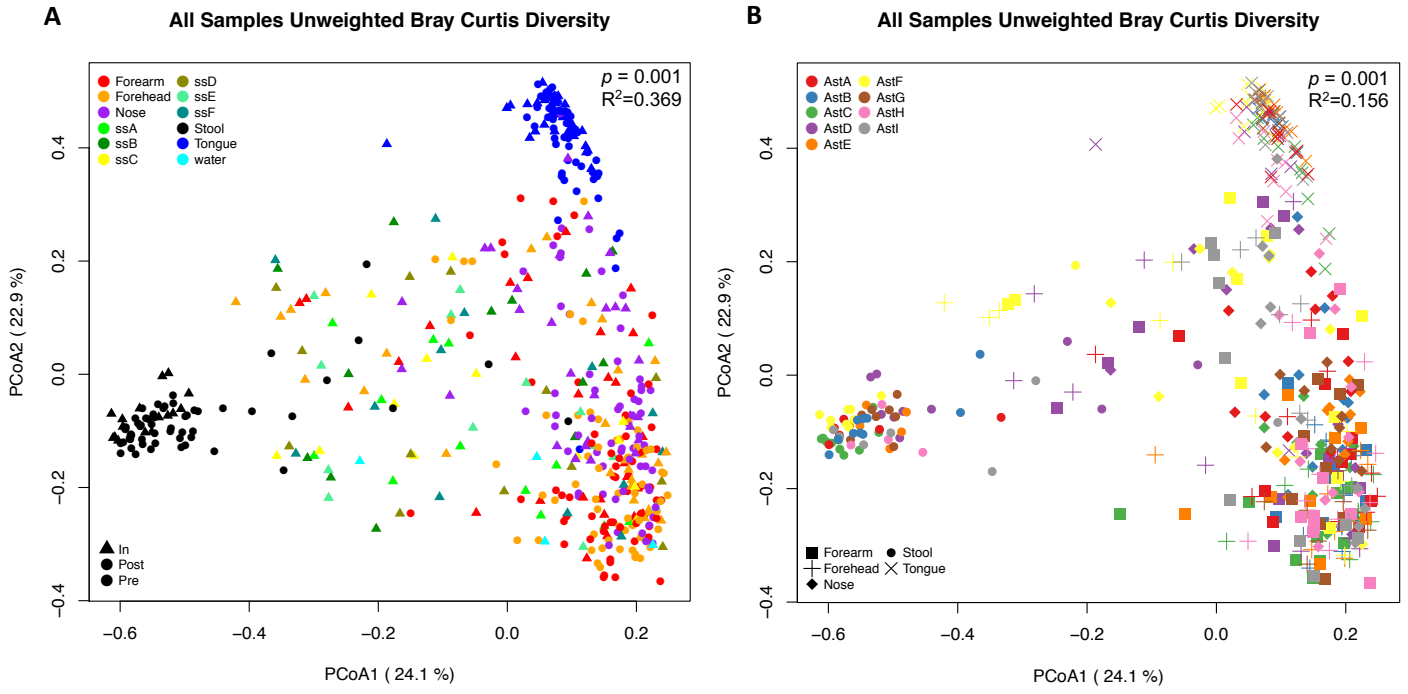


Figure S2

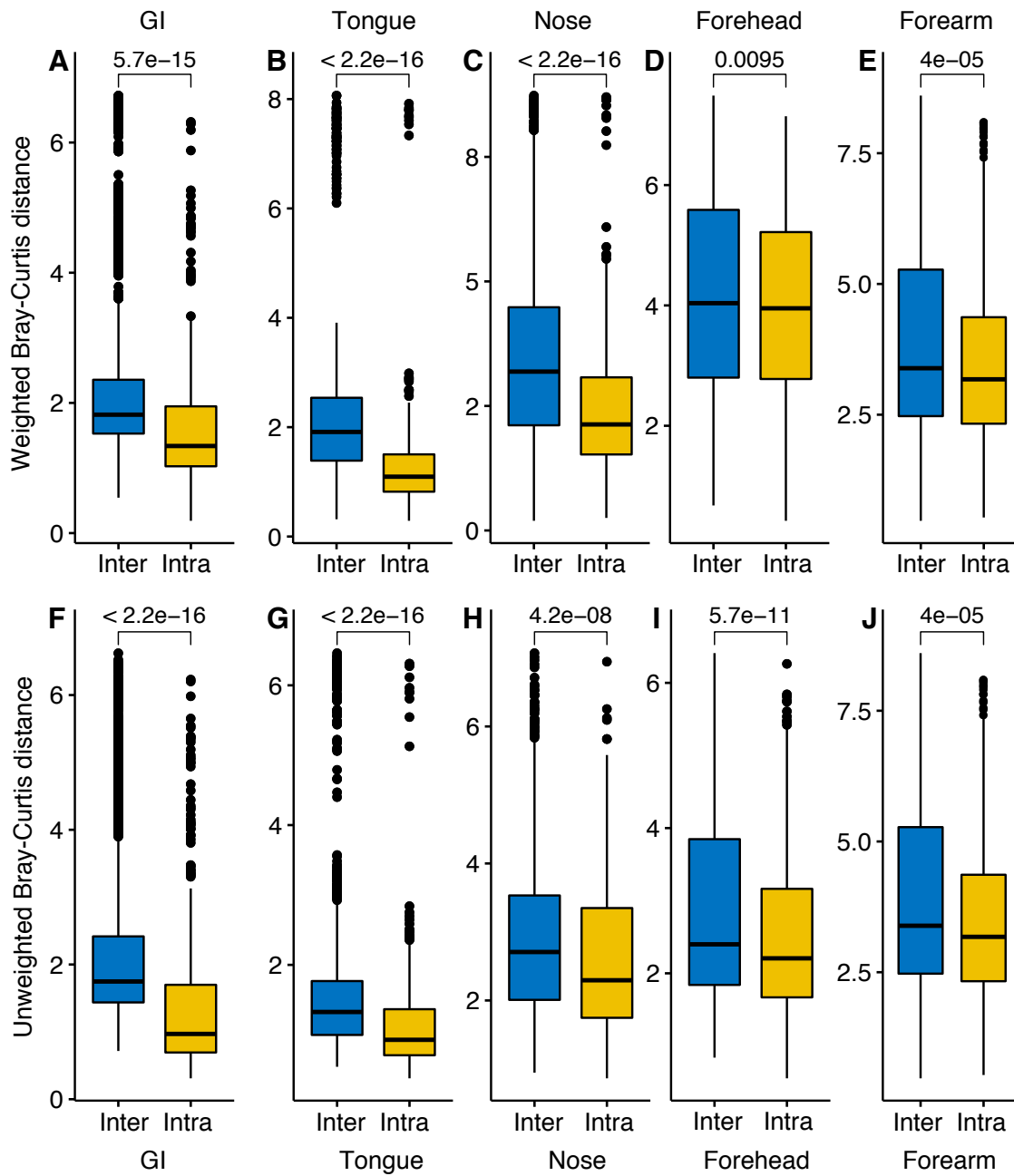


Figure S3

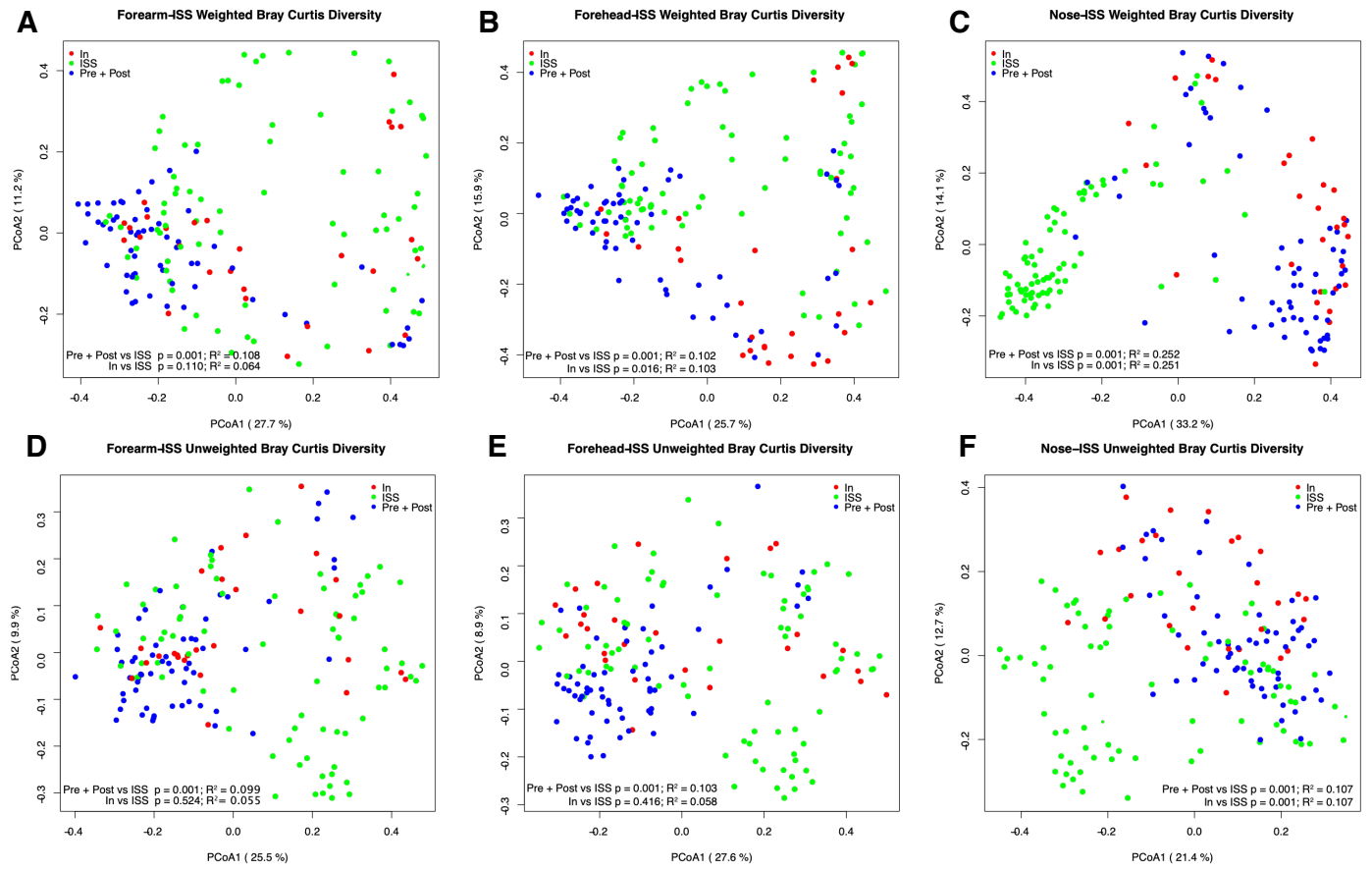


Figure S4

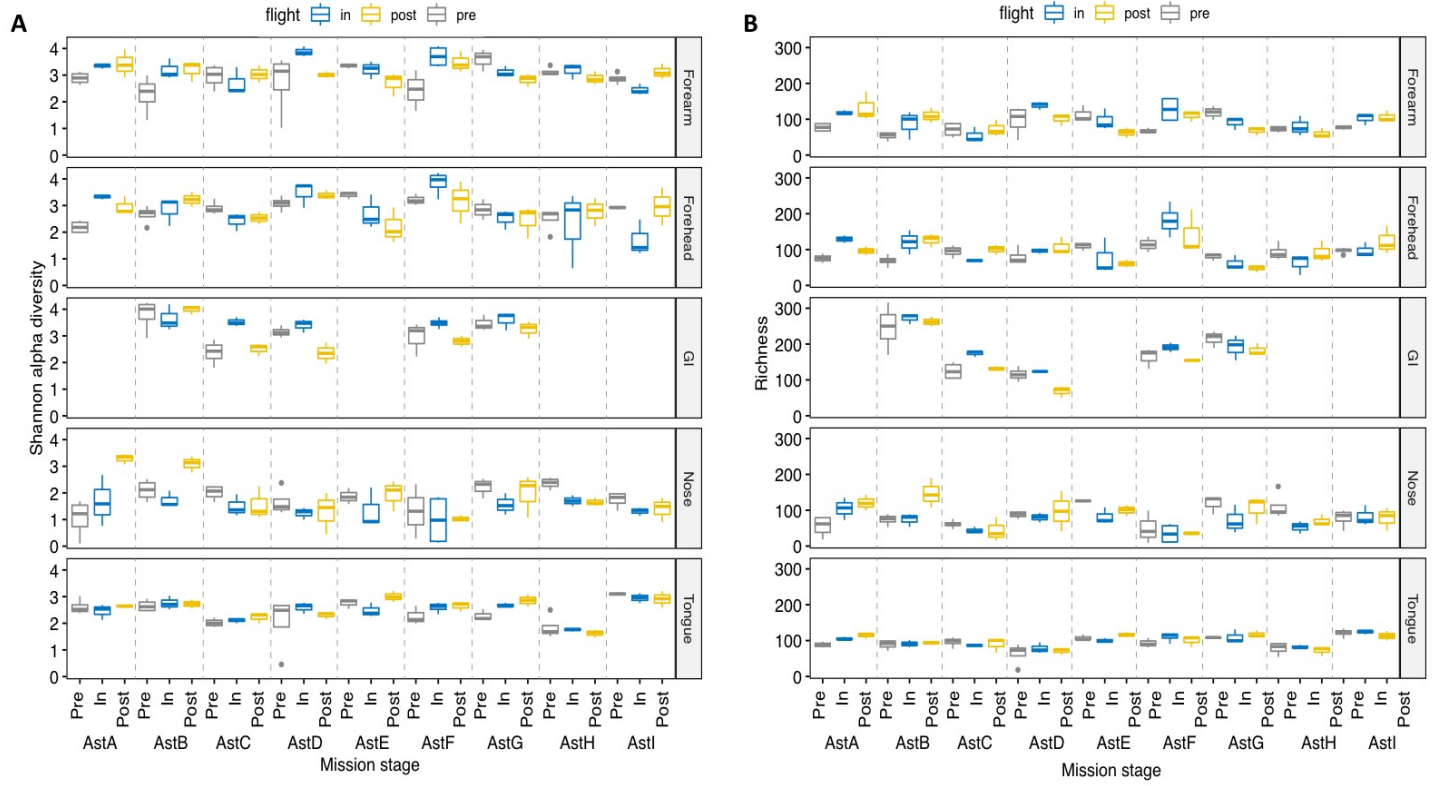


Figure S5

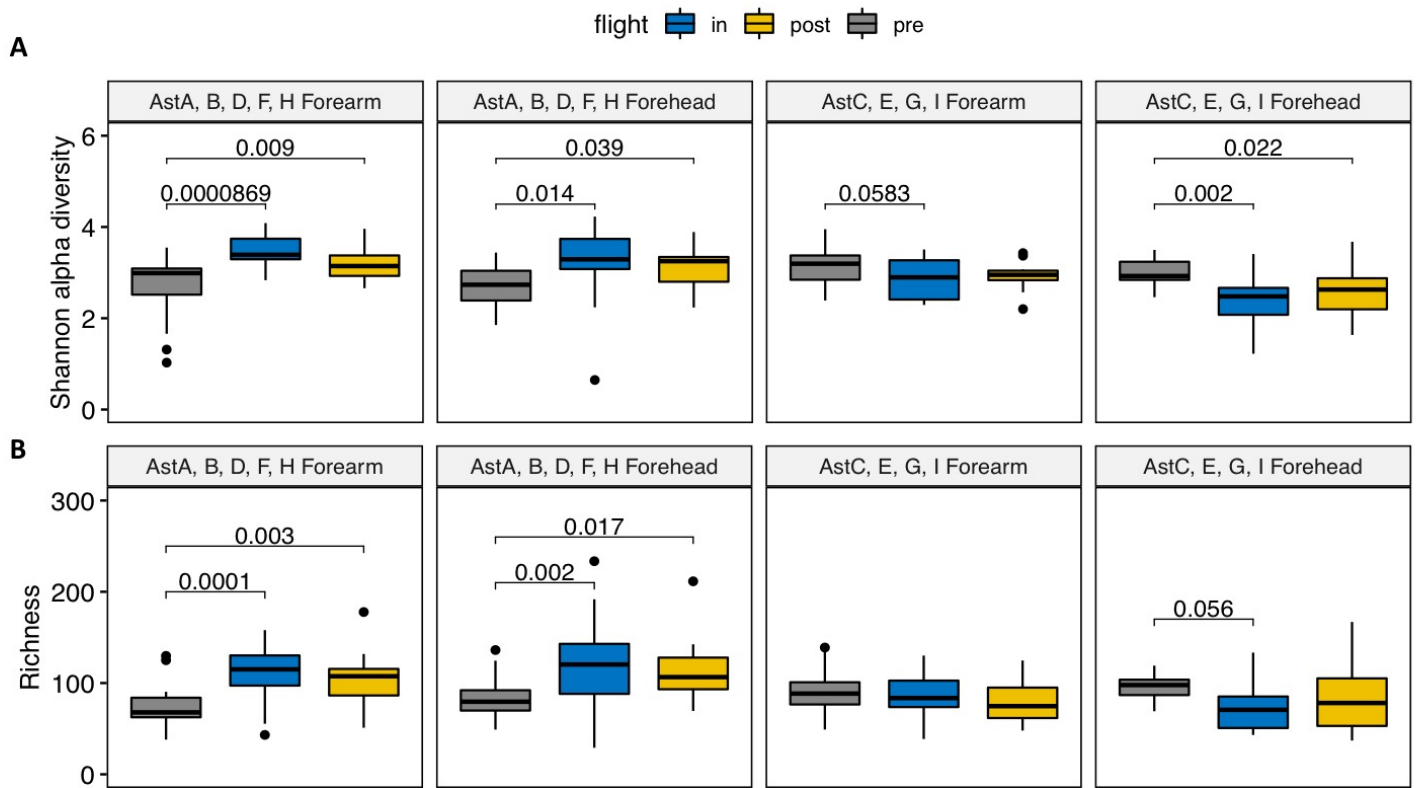


Figure S6

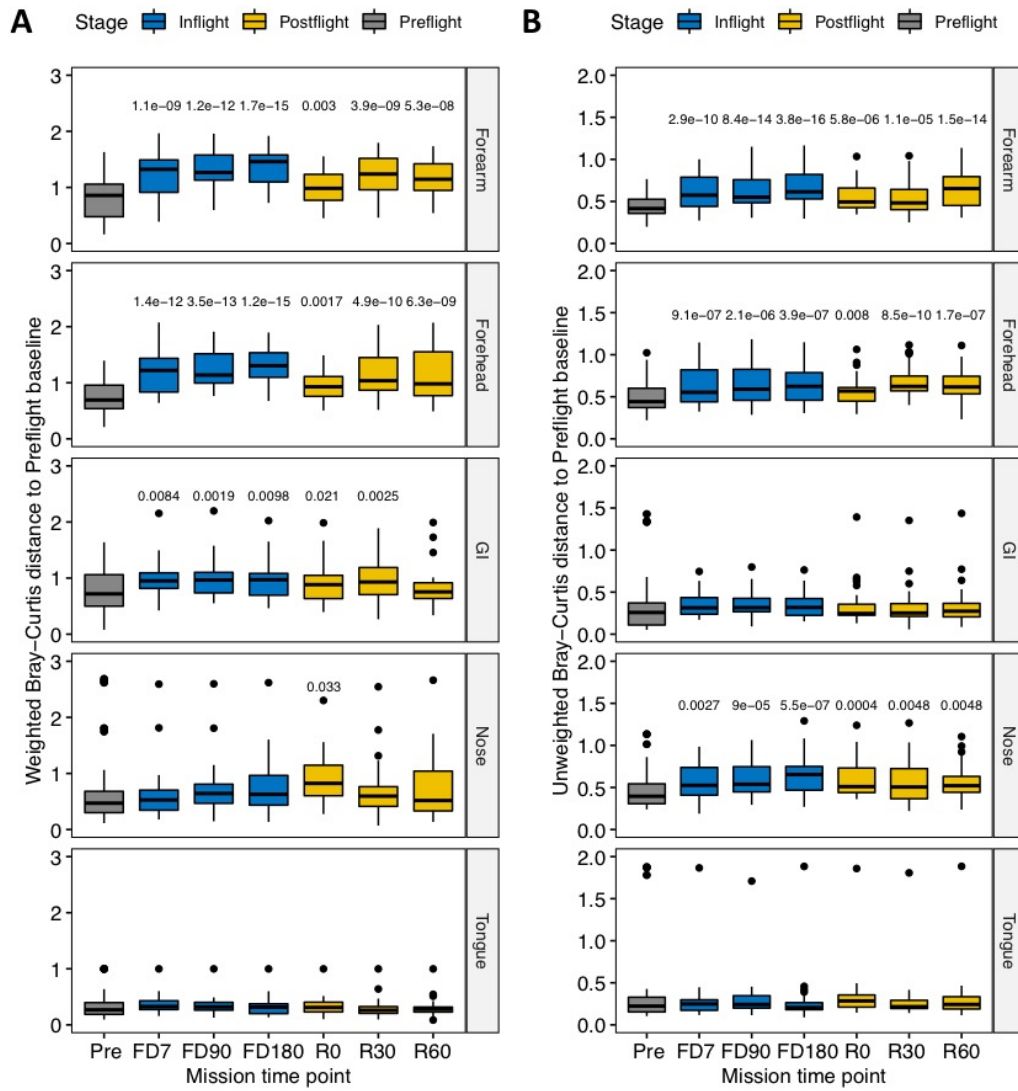


Figure S7

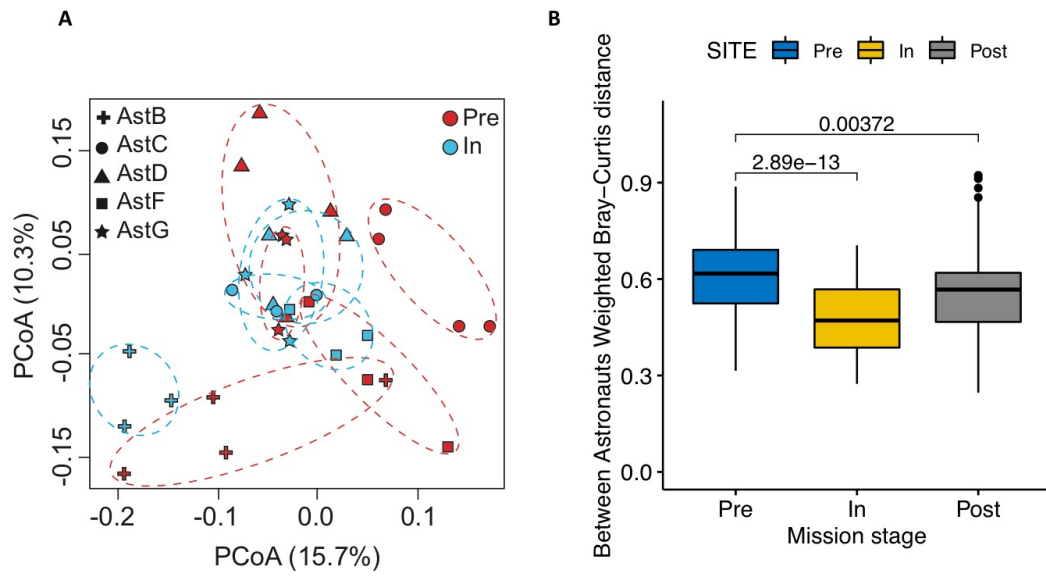


Figure S8

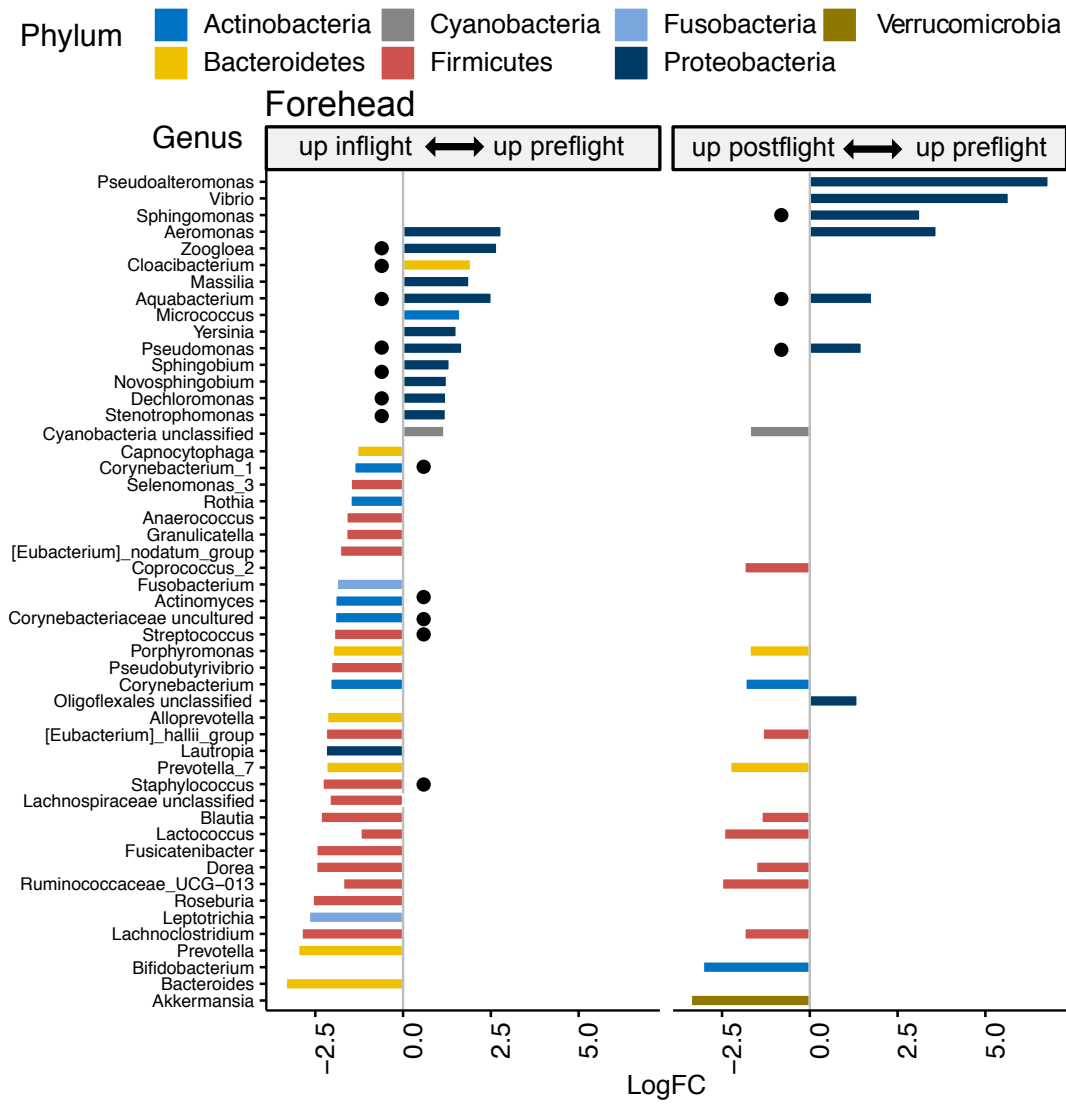


Figure S9

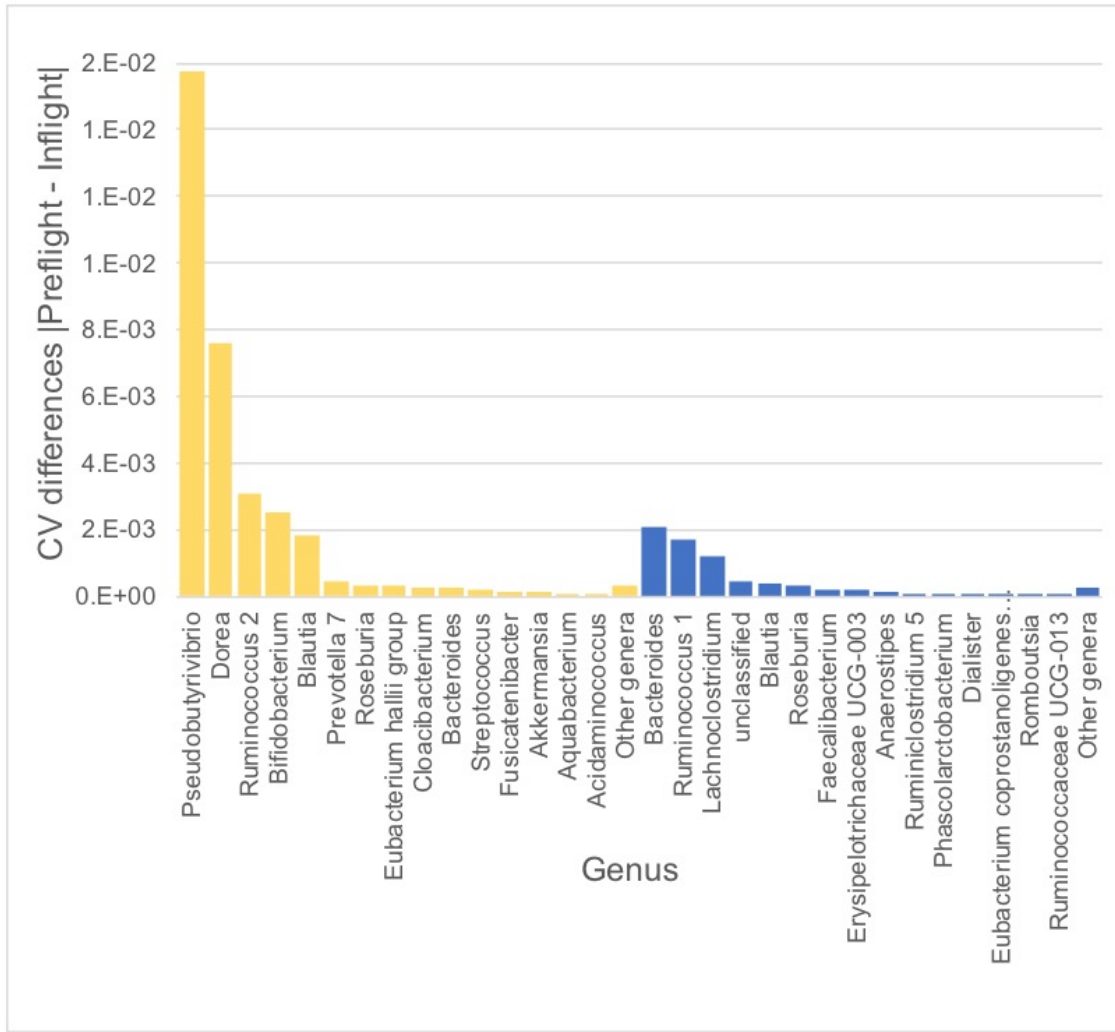


Figure S10

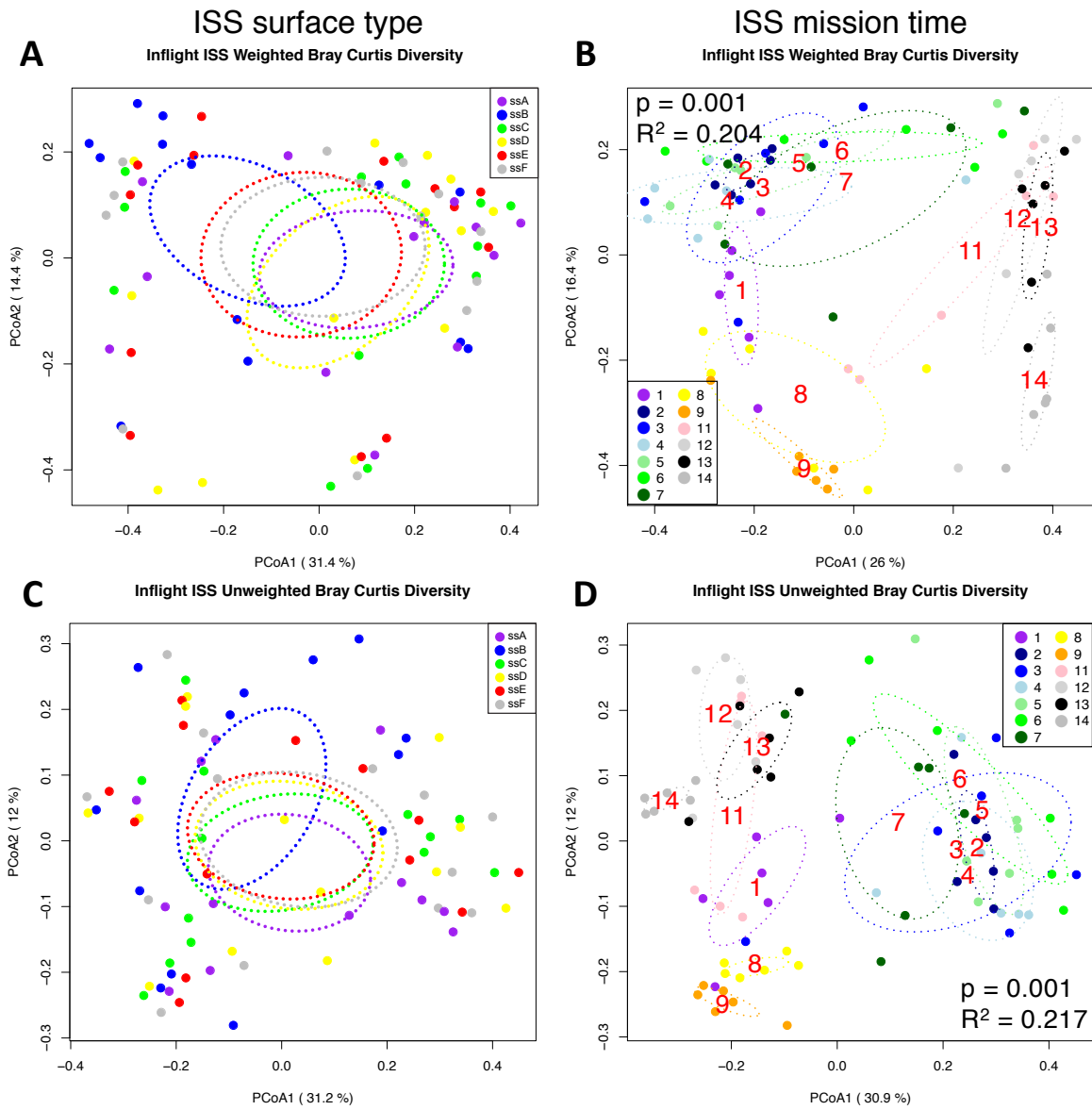
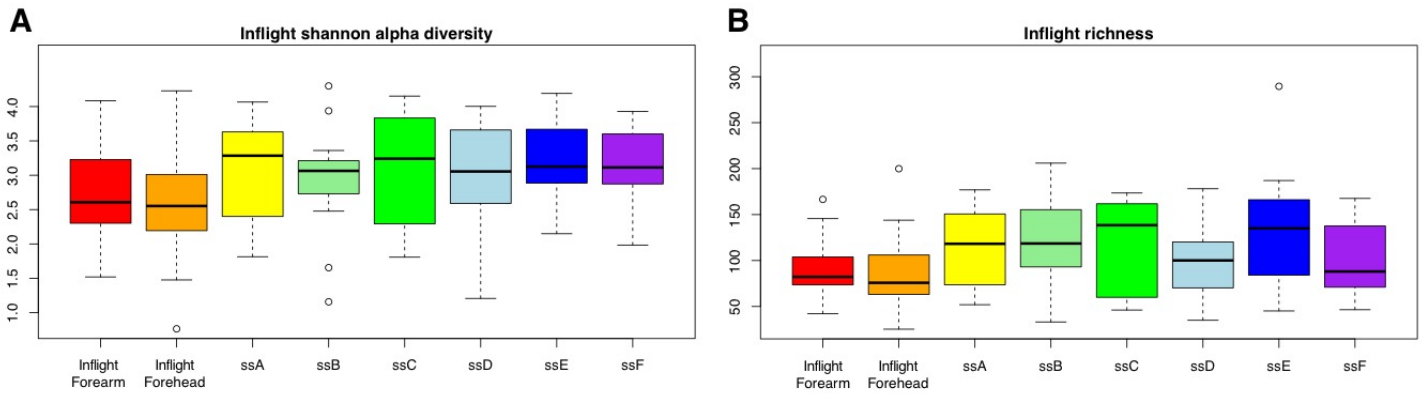


Figure S11



ISS surfaces sampled:

- ssA:** ARED Handle Bar
- ssB:** Intermodular Ventilation (IMV) Inlet
- ssC:** Cupola Nadir Window Shade Knob

- ssD:** Crew Quarters Stationary Light Knob
- ssE:** Smoke Detector
- ssF:** Handheld Microphone handle/grip

Figure S12

OTUs not missing two consecutive time points at ISS site siteA

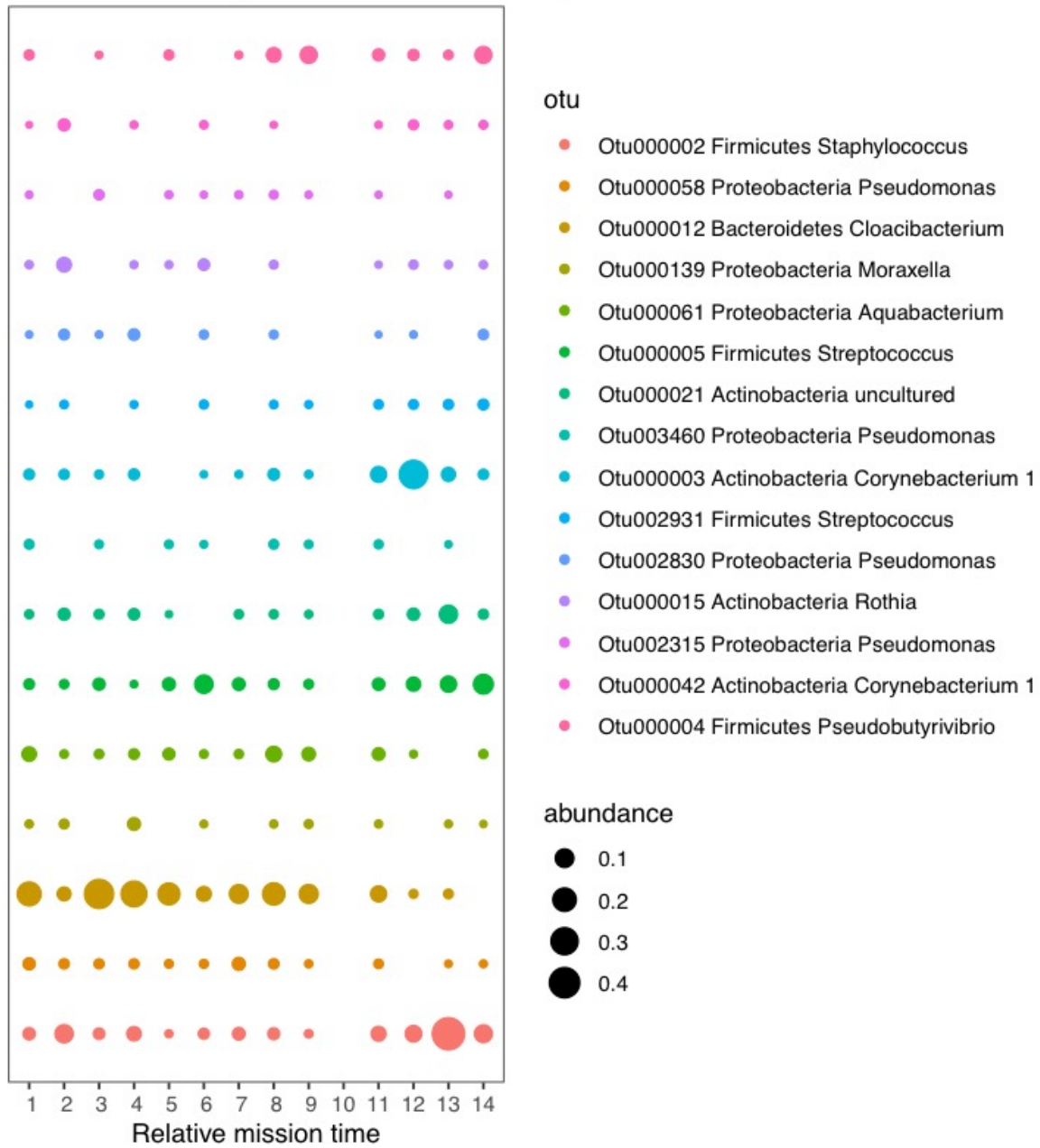


Figure S13

OTUs not missing two consecutive time points at ISS site siteB



Figure S14

OTUs not missing two consecutive time points at ISS site siteC

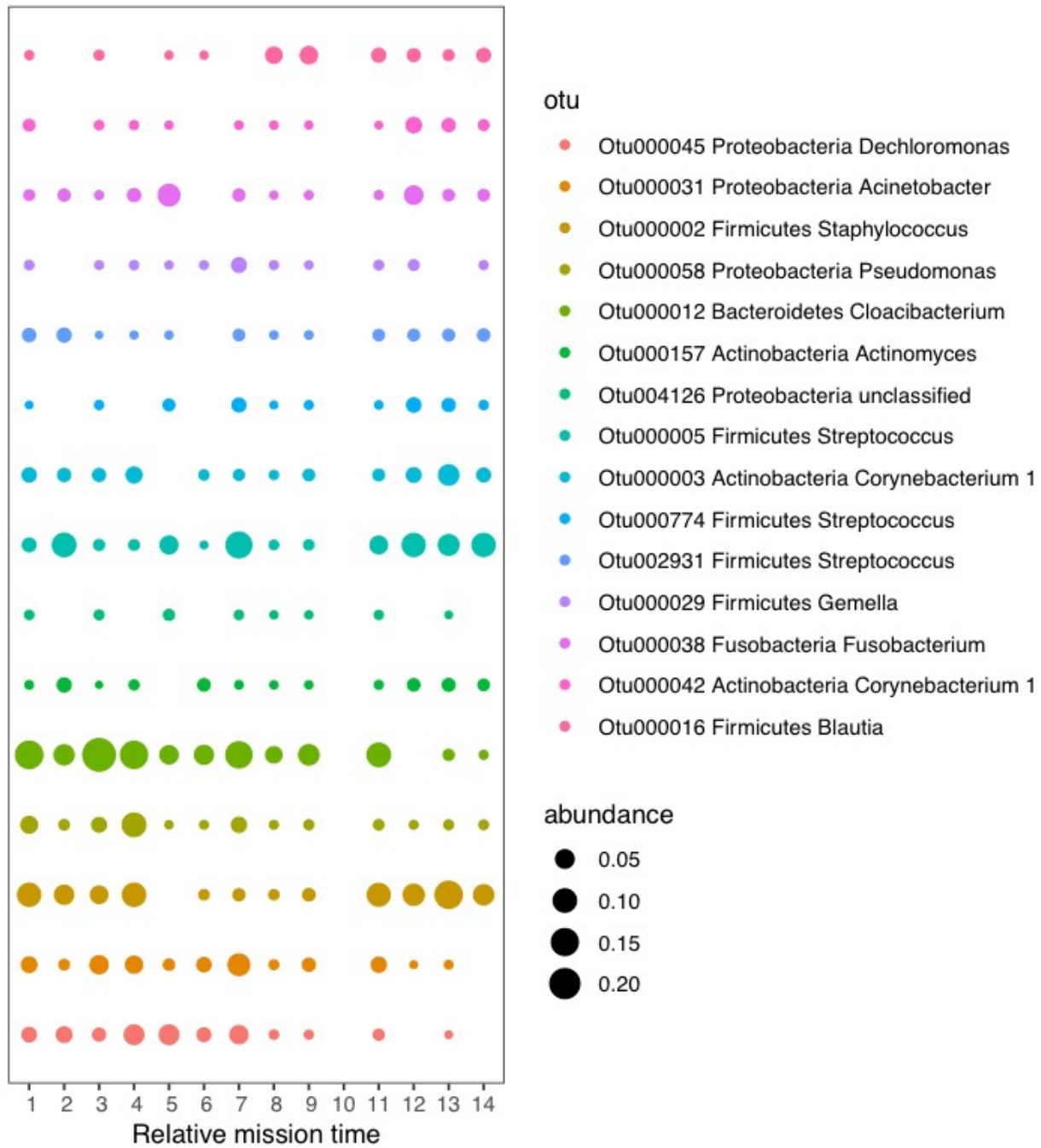


Figure S15

OTUs not missing two consecutive time points at ISS site siteD

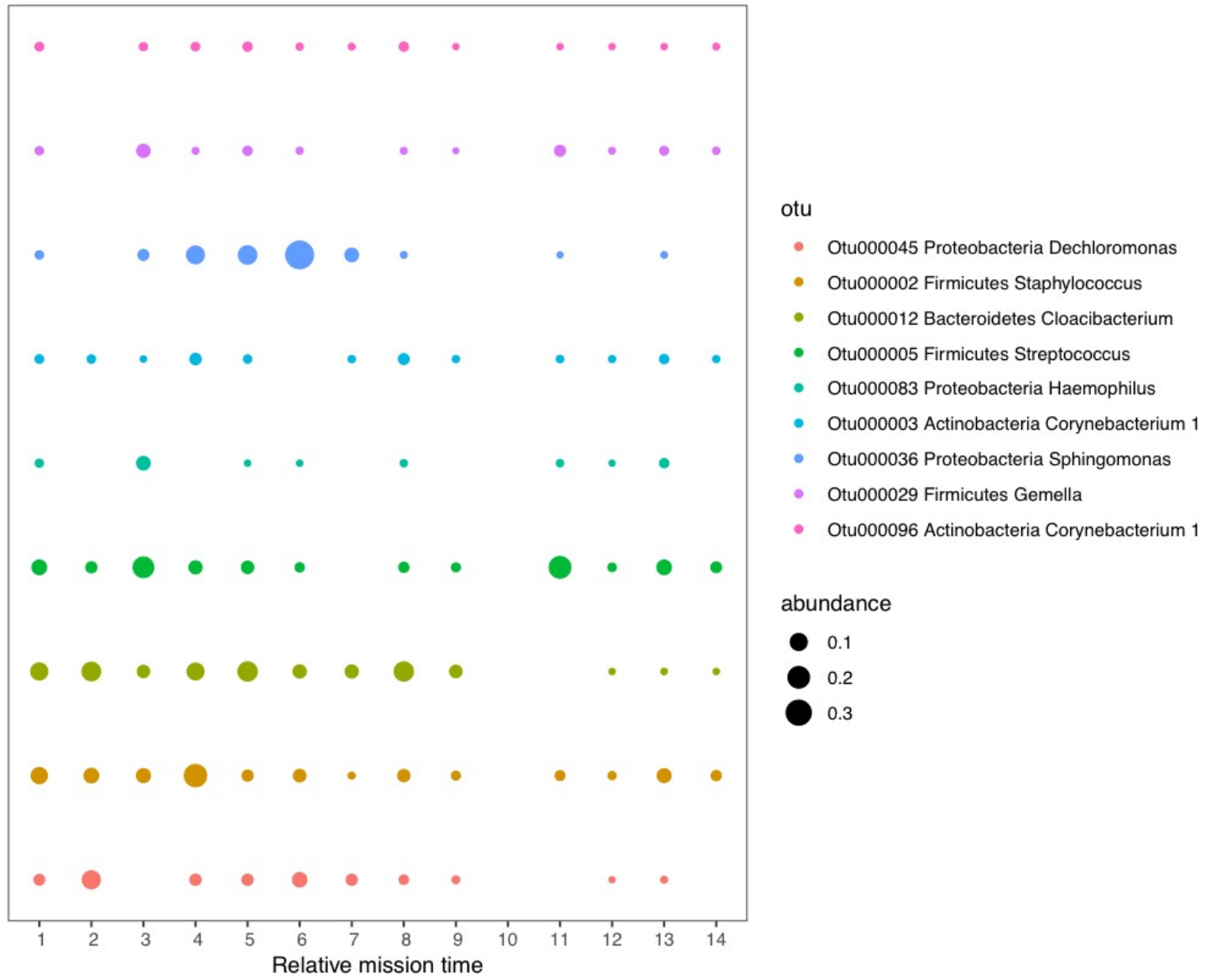


Figure S16

OTUs not missing two consecutive time points at ISS site siteE



Figure S17

OTUs not missing two consecutive time points at ISS site siteF

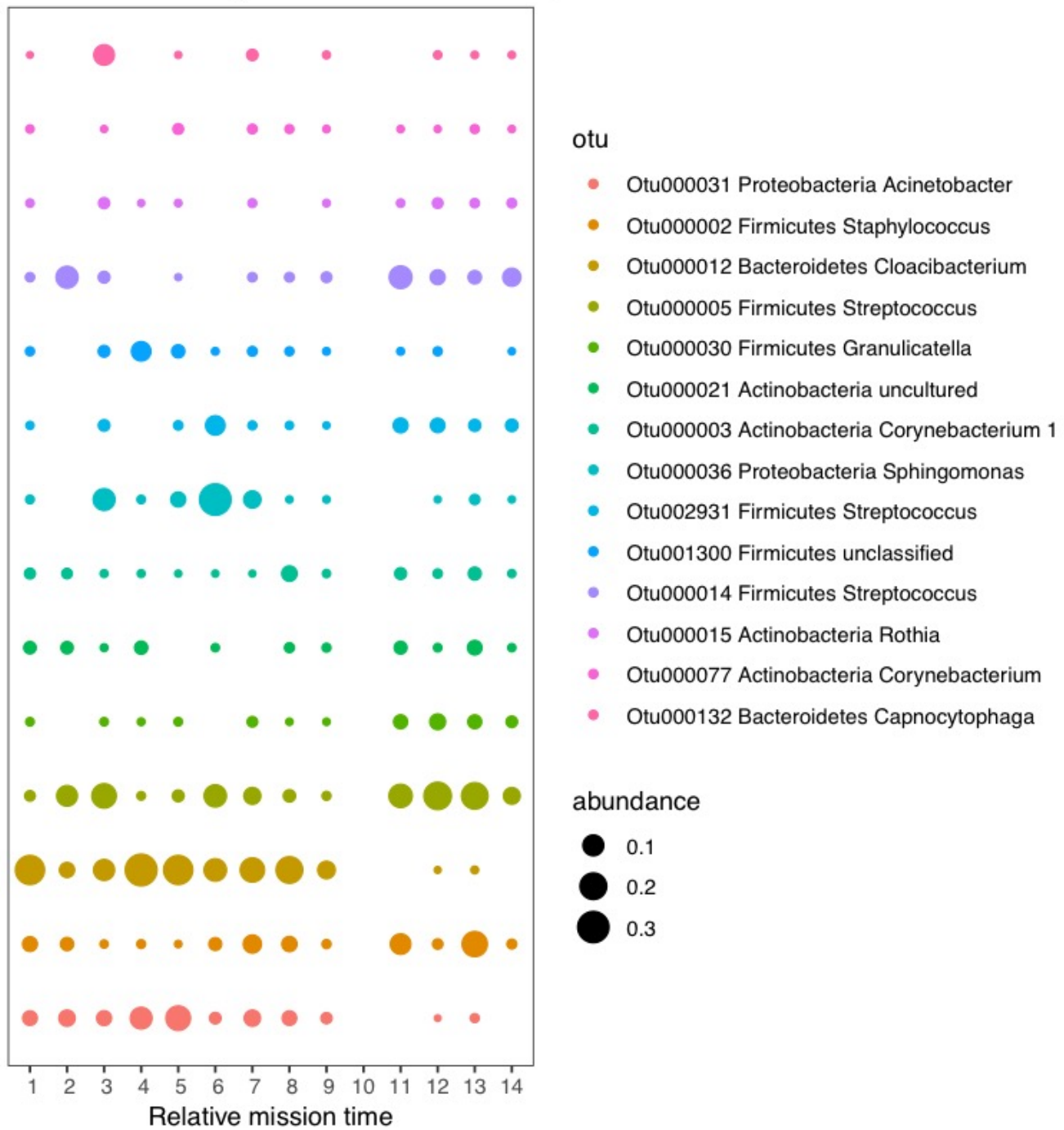


Figure S18

